

A Novel In Vitro Preparation: the Intact Hippocampal Formation

Neurotechnique

Ilgam Khalilov,* Monique Esclapez,* Igor Medina, Djamilia Aggoun, Karri Lamsa, Xavier Leinekugel, Roustem Khazipov, and Yehezkel Ben-Ari†
INSERM U 29
Hôpital de Port Royal
75014 Paris
France

Summary

The intact hippocampal formation (IHF) of neonatal or young rats can be kept alive for an extended period in a fully submerged chamber with excellent morphological preservation. Field or patch-clamp recordings, intracellular Ca^{2+} measurements, and 3-D reconstruction of biocytin-filled neurons can be performed routinely. The generation and propagation of network-driven activities can be studied within the IHF or between connected intact structures such as the septum and the hippocampus or two hippocampi, and the use of a dual chamber enables the application of drugs separately to each structure. This preparation will be useful to study intact neuronal networks in the developing hippocampus *in vitro*.

Introduction

Studies using acute brain slices *in vitro* have contributed greatly to our understanding of brain mechanisms. The principal advantages offered by slice preparations are the abilities to control the external medium, to apply known concentrations of drugs, and to record from identified layers (Aitken et al., 1995) or visually identified neurons (Stuart et al., 1993). However, more complex *in vitro* preparations in which the neuronal network is not damaged, as it is in slices, are clearly required in order to study the generation and propagation of synchronized neuronal activities. To overcome this problem, a number of *in vitro* intact noncortical brain structure preparations have been introduced, mainly in the field of developmental neurobiology (Otsuka and Konishi, 1974; Bourque and Renaud, 1984; Fulton and Walton, 1986; O'Donovan, 1989; Frank, 1993; Gu and Spitzer, 1995; Cazalets et al., 1996; Jacquin et al., 1996; Mooney et al., 1996). For mammalian cortical structures, an elegant development was recently provided by Llinas and colleagues, who described a procedure that allows the isolation and maintenance of a perfused adult guinea pig brain *in vitro* (De Curtis et al., 1991; Muhlethaler et al., 1993; Pare and Llinas, 1995). This preparation cannot, however, be used in small animals (mice or young rats) because of the size of the vertebral arteries and does not provide the advantages for performing pharmacological manipulations that slice preparations offer.

We now describe a simple *in vitro* experimental system allowing conventional recordings of the neonatal intact hippocampal formation (IHF), or of a complex including the two hippocampi and the septum in a submerged chamber, that offers most of the advantages of slices, namely, the use of the entire repertoire of electrophysiological, morphological, pharmacological, and imaging techniques. This preparation offers unique advantages for 3-D morphological reconstruction of individual neurons and for the study of generation and propagation of a variety of network activities (paroxysmal discharges, giant depolarizing potentials, etc.). This approach should be very useful for the study of physiological and pathological network activities in the developing cortical neuronal ensembles.

Results

Morphological Aspect of the IHF *In Vitro*

Light microscopy experiments demonstrated that the general histological characteristics of the hippocampal formation and the morphology of the vast majority of neurons, including interneurons, were well preserved in the IHFs from immature rats (postnatal days 0–10 [P0–P10]) maintained *in vitro* for up to 10 hr and in the IHFs from P15 animals maintained *in vitro* for up to 4 hr (Figure 1). On cresyl violet-stained sections obtained throughout the rostrocaudal extent of the IHF, the cell bodies of principal cells formed a continuous band in the pyramidal and granular cell layers (Figure 1A). Numerous neurons were present in the hilus, and many neuronal cell bodies were dispersed in all hippocampal layers (Figure 1A). On thin sections, the cell bodies of pyramidal neurons in the CA1 (Figures 1B and 1D) and CA3 (Figure 1E) regions were densely packed and exhibited a well-formed nucleus surrounded by a thin shell of cytoplasm. Their dendrites, extending throughout the stratum radiatum and stratum oriens, were clearly observed. In these dendritic layers, the cell bodies of several interneurons were present and morphologically healthy. Only a few cell death profiles, including swollen neurons or shrunken dark cells, were present in CA1 and CA3 regions. These profiles were observed more frequently at P10–P15 than at P0–P10 but were rare as compared to age-matched hippocampal slices processed in the same condition, in which, in keeping with earlier studies (Aitken et al., 1995), many degenerating cells were present (Figure 1E). After more than 10 hr *in vitro*, all IHFs, including those observed at P0–P10, exhibited many cell death profiles and large extracellular spaces indicating damaged tissue.

Electron microscopy experiments in preparations kept *in vitro* for 4 hr confirmed and extended the excellent morphological preservation of neurons in the IHF. Well-defined membranes limited all cellular elements, including cell bodies and dendrites of neurons. The somata of pyramidal neurons were usually clustered together with their plasma membranes closely apposed (Figure 2A). These perikaryons displayed a large, round nucleus with homogeneous dispersed karyoplasm and a large,

* These authors contributed equally to this work.

† To whom correspondence should be addressed.

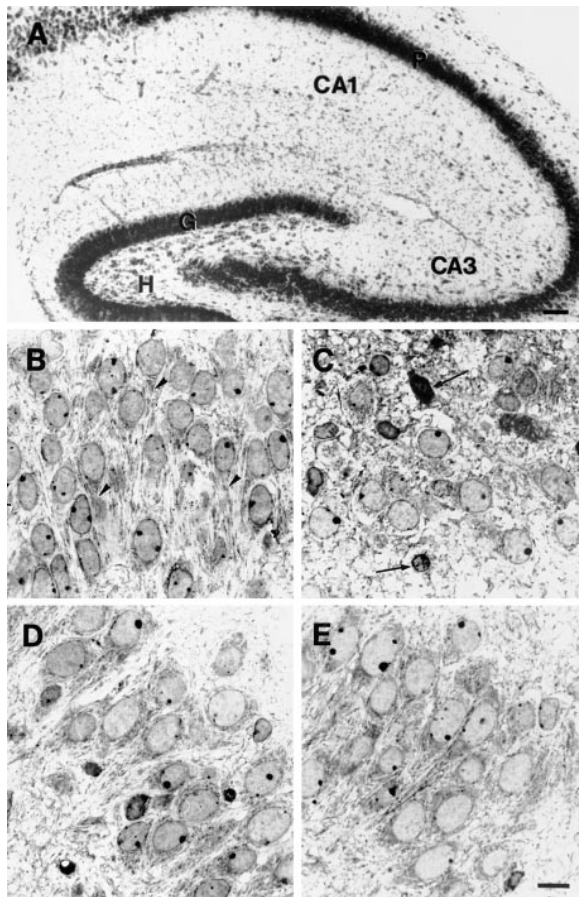


Figure 1. Light Microscopic Histological Characteristics of the Rat Intact Hippocampal Formation (IHF) In Vitro

(A) Cresyl violet-stained section (40 μm) of P15 IHF maintained for 4 hr in vitro demonstrates the well-preserved organization, in continuous bands, of pyramidal cells (P) in the CA1 and CA3 regions and of granular cells (G) in the dentate gyrus. Note the presence of numerous neurons in the hilus (H) as well as many neurons dispersed in all hippocampal layers.

The remaining panels illustrate, in thin sections (1–2 μm) stained with toluidine blue, the features of the tissue in the various hippocampal fields from IHF ([B], [D], and [E]) and from a slice processed in the same condition (C).

(B) At P5, CA1 pyramidal neurons are densely packed and are healthy morphologically. The soma of these neurons displays a round, clear nucleus surrounded by thin shell of cytoplasm. Proximal dendrites emerging from the soma are observed (arrows).

(C) In contrast, in a slice (P5) processed under the same conditions, morphologically healthy CA1 pyramidal neurons are more dispersed and extracellular spaces are large (compare [C] to [A]). Note also the presence of several degenerating shrunken dark cells (arrows). (D–E) At P10, the morphology of pyramidal neurons is preserved in the CA1 (D) and CA3 (E) regions. This preservation of tissues is similar in young animals (P10) and neonatal preparations (compare [D] and [E] to [B]).

Scale bars: (A) 100 μm ; (B–E) 10 μm .

dense nucleolus (Figures 2A and 2B). All organelles found in neurons were present in the cytoplasm (Figure 2B). Axon terminals making synaptic contacts with the soma and dendrites of pyramidal cells were observed. The neuropil and the extracellular spaces were also well preserved, in comparison to age-matched hippocampal slices processed in the same conditions (compare Figures 2A–2B with Figure 2C; also see Aitken et al., 1995),

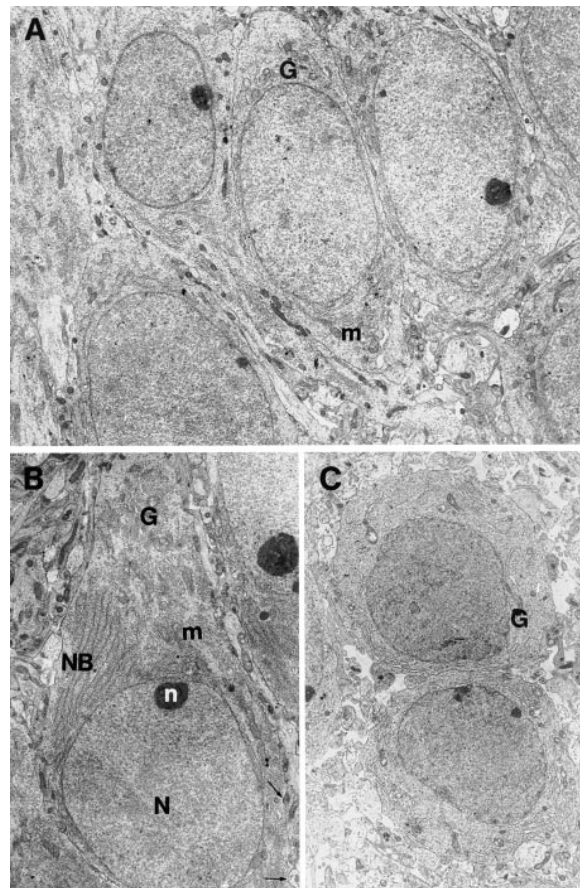


Figure 2. Electron Microscopic Morphological Characteristics of IHFs

IHF of P5 (A) and P10 (B) rats as well as a P5 hippocampal slice (C) were maintained in vitro for 4 hr.

(A) CA1 neurons are clustered together with their plasma membranes closely apposed. Well-defined membranes limit all cellular and subcellular elements. Note the good preservation of the neuropil and extracellular spaces.

(B) Cell body and apical dendrite of a CA3 pyramidal neuron. Most of the perikaryon is occupied by a large round nucleus (N) that displays a dense nucleolus (n) and a homogeneous dispersed karyoplasm. The cytoplasm surrounding the nucleus contains many organelles, including Nissl bodies (NB), Golgi apparatus (G), and mitochondria (m). Note also axon terminals that synapse with the cell body (arrows).

(C) In contrast, in a slice (P5) prepared under the same conditions, large extracellular spaces and dissociated neuropil are observed in the CA1 region (compare [C] to [A]).

Magnification, 2250 \times .

and were similar to those described after in situ fixation (Peters et al., 1991).

The morphological quality of P0–P15 IHFs was further confirmed by glutamic acid decarboxylase (GAD) immunohistochemistry. In keeping with previously reported data in rats fixed in situ (Rozenberg et al., 1989; Dupuy and Houser, 1996), GAD-labeled neurons and terminals were distributed in all layers of the hippocampal formation at P10–P15, including the principal cell layers of the hippocampus and dentate gyrus, whereas GAD-containing fibers and cell bodies occupied almost exclusively the dendritic regions and were almost absent in the principal cell layers in P0–P3 IHFs (data not shown).

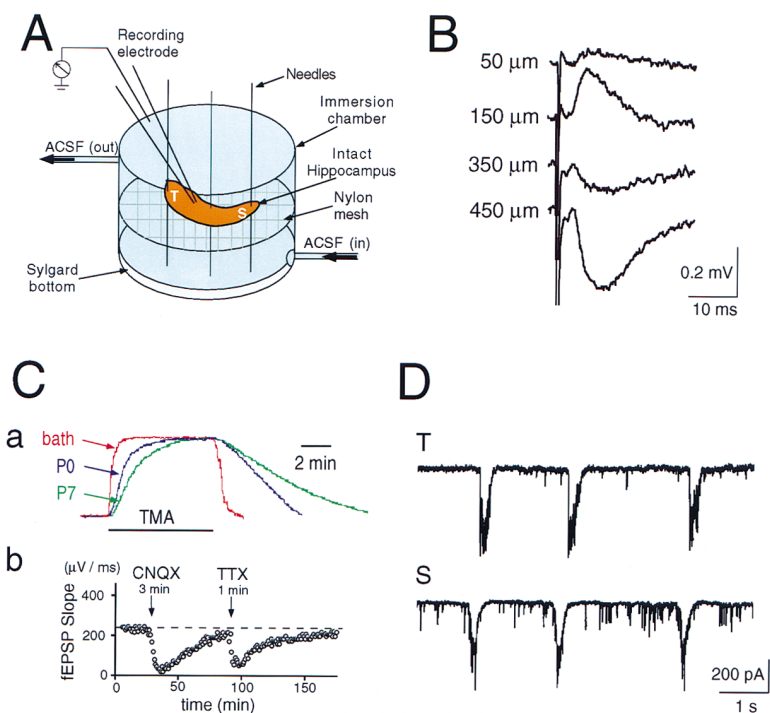


Figure 3. Electrophysiological Properties of IHF In Vitro

(A) Scheme of the recording chamber. (B) Extracellular field potential responses evoked in CA1 region by electrical stimulation of Schaffer collaterals were recorded at the different depths of the P7 IHF. Note that field EPSPs reverse at the level of the pyramidal layer. (C) Rate of wash in and wash out of bath applied drugs in the IHF. (a) Normalized changes of TMA^+ activity in the bath (red curve) and in the core of the IHF of P0 (blue curve) and P7 (green curve) rats in response to TMA bath application (solid bar). (b) Bath application of the AMPA receptor antagonist CNQX ($10 \mu M$ for 3 min) or TTX ($1 \mu M$ for 1 min) reversibly blocked field EPSPs. (D) In IHFs from P0–P6 rats, spontaneous GDPs were regularly observed. Dual recordings from temporal (T) and septal (S) poles of IHF revealed a significant delay of propagation of GDPs.

Electrophysiological Properties of the IHF

The electrophysiological properties of the P0–P10 IHFs were assessed using field potential and whole-cell patch clamp recordings. Electrical stimulation of the Schaffer collaterals evoked typical field excitatory postsynaptic potentials (EPSPs) in the CA1 region that were preceded by an afferent volley and had a latency, duration, and laminar profile similar to that observed in vivo and in slices (Figure 3B). These EPSPs were reversibly blocked by tetrodotoxin (TTX; $1 \mu M$) or the AMPA receptor antagonist CNQX ($10 \mu M$) (Figure 3Cb).

Whole-cell recordings were routinely performed either blindly or under visual control using infrared microscopy (Figure 4A). The mean resting potential was -62 ± 4 mV ($n = 74$), and cells fired overshooting action potentials in response to depolarizing steps. Moreover, the characteristic giant depolarizing potentials (GDPs; Ben-Ari et al., 1989) that result from the synchronous discharge of pyramidal cells and interneurons (Khazipov et al., 1997; Leinekugel et al., 1997) were recorded from pyramidal cells and interneurons ($n = 55$ of 61 IHFs; see below) with a similar frequency ($7 \pm 3 \text{ min}^{-1}$; $n = 12$ IHFs) as in slices (Ben-Ari et al., 1989). Dual recordings in the rostral and caudal poles of the IHF or in the two interconnected hippocampi allow one to study the site of generation and propagation of GDPs (Figure 3D).

Interestingly, the latencies of antagonist effects were similar to those observed in age-matched slices in the same chamber, suggesting fast diffusion rates of drugs into the IHF. To assess the diffusion rate in the core of the IHF, TMA^+ activity measurements were performed using TMA^+ -sensitive electrodes. As shown in Figure 3Ca, the response to TMA^+ bath application (0.5 – 5 mM) was well fitted by single-exponential functions with time constants of $\tau_{in} = 24 \pm 1$, 84 ± 1 , and 135 ± 7 s and $\tau_{out} = 42 \pm 1$, 310 ± 14 , and 400 ± 28 s in the bath and in the core of P0 and P7 IHFs, respectively ($n = 6$). Thus,

basic properties of both pyramidal cells and interneurons are not affected in the IHF, and pharmacological studies can be readily performed.

Stable field EPSPs were routinely recorded for durations of 6–10 hr ($n = 54$); in four experiments, field EPSPs were recorded in IHFs that had been kept in vitro for 20–24 hr. Therefore, it is possible to study the long term effects of procedures that generate persistent changes in synaptic transmission. Thus, $1 \text{ Hz} \times 15 \text{ min}$ and $100 \text{ Hz} \times 1 \text{ s}$ stimulation protocols generated LTD or LTP of the field EPSP, respectively (H. Gozlan, personal communication).

In contrast to P0–P10 IHFs, synaptic activity was strongly depressed in IHFs from older animals. Thus, field EPSPs were obtained in only 3 out of 12 IHFs at P12 and in none at P15 ($n = 9$ IHFs). This precludes the routine use of IHFs older than P10 for electrophysiological experiments. Age limitations are likely due to a reduction of the diffusion rate with age (Figure 3C) and, therefore, to hypoperfusion in the core of the IHFs of older animals. Indeed, pH measurements revealed that, whereas the pH values in the core of the IHFs were in the physiological range until P10, there was a significant acidosis up to 6.7 (6.81 ± 0.05 ; $n = 5$) in P11–P15 IHFs. However, neurons were successfully labeled with biocytin via patch electrodes and processed for 3-D reconstruction in P15 IHFs ($n = 3$).

Unique Features of the IHF Preparation

The IHF is particularly useful for complete morphological characterization of neurons and for the study of the generation and propagation of network activities within the hippocampus, in the septo-hippocampal system, or between the interconnected hippocampi.

Morphological Features and 3-D Reconstruction of Biocytin-Filled Neurons

The entire axonal and dendritic arborizations of pyramidal cells (Figure 5A) and interneurons (Figure 5B) could

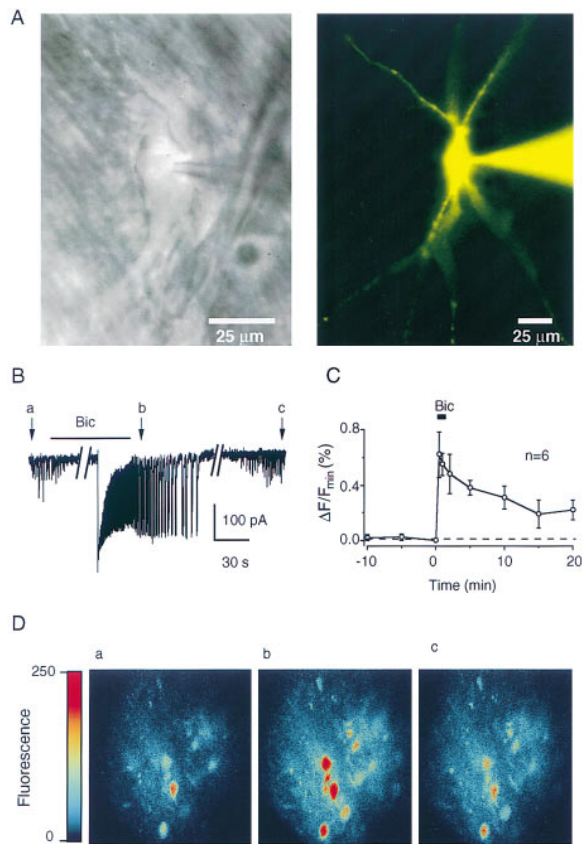


Figure 4. Visualization of Neurons Using Infrared Microscopy and Confocal Imaging in the IHF

(A) Stratum oriens interneuron visualized using infrared microscopy in IHF from P6 rat (left). On the right, fluorescent image of the same neuron loaded by Lucifer yellow via whole-cell pipette.

(B–D) Simultaneous recordings of electrical activity (B) and calcium fluorescence ((C) and (D)) during ictal-like activity induced by blockade of GABA_A receptors.

(B) Trace of bicuculline-induced (10 μ M) ictal-like discharge recorded from a CA1 pyramidal neuron in the same IHF shown in (D), with indications of the moments (arrows a, b, and c) when the images were scanned.

(C) Average of the fluorescence changes induced by bicuculline in six IHFs taken from P6–P7 rats.

(D) Pseudocolor images in the plane of CA1 pyramidal cells loaded with Ca²⁺-sensitive dye Fluo 3-AM were obtained in control (a), during the ictal phase of bicuculline response (b), and after 20 min of washing with bicuculline (c).

be labeled and processed for 3-D reconstruction in IHFs from P0–P15 animals (Figure 5C). The CA1 stratum oriens interneuron illustrated in Figure 5B displayed an extensive dendritic and axonal arborization, somewhat similar to the observations made in vivo (Freund and Buszaki, 1996). Unexpected from studies in conventional slices, several axonal branches were frequently running over 1 mm throughout the whole hippocampal structure (Figure 5C).

Intra-Hippocampal Recordings

As mentioned above, generation and propagation of network-driven activities, such as GDPs (see above) or epileptiform discharges, can be studied with multiple site recordings. Thus, long-lasting ictal discharges (30–

250 s) were readily induced by bicuculline (Figure 4B), kainate (Figure 6D), high K⁺ solution (Figure 6E; see below), or kindling (data not shown). These results contrast with the brief interictal activities observed in age-matched slices in the same conditions (data not shown). [Ca²⁺]_i changes associated with epileptiform activity could also be monitored in the IHF using confocal microscopy from groups of neurons loaded extracellularly with Fluo 3-AM (Figures 4C and 4D).

The Septo-Hippocampal Pathway

In the intact septo-hippocampal complex in vitro, electrical stimulation of the septum inhibited the firing of hippocampal CA3 stratum oriens interneurons (Figure 6C), in keeping with the GABAergic projections from the septum to hippocampal interneurons (Freund and Antal, 1988; Toth et al., 1997). Furthermore, as suggested previously from in vivo data (Tremblay et al., 1984), bath application of kainic acid (250 nM) generated an ictal discharge (Figure 6D) in P4 IHFs. This originates from the hippocampus and propagates to the septum, since it is abolished in the septum by surgical separation from the hippocampus (data not shown).

The Commissural Connections

Synchronous field or dual whole-cell recordings from the two interconnected hippocampi were routinely performed. To study more thoroughly the propagation of events from one hippocampus to the other, we developed a dual chamber that enabled us to perfuse the two interconnected hippocampi with different artificial cerebrospinal fluids (ACSFs; Figure 6B). Thus, unilateral application of high Mg²⁺ ACSF (7–9 mM; Figure 6E) or TTX (1 μ M) blocked the propagation of the ictal discharge generated in the contralateral hippocampus by high K⁺ (7.5 mM) solution (Figure 6E).

Discussion

Our results suggest that it is possible to use, in the intact hippocampus, the entire repertoire of techniques that have made hippocampal slices so useful and popular, including bath application of drugs, full control of fluid environment (temperature, pH), infrared and fluorescence imaging, calcium measurements, and so on. It also provides a most convenient way for the morphological study of the neuronal organization of the hippocampus, even in neonates in which in situ intracellular recordings and 3-D reconstruction have not been performed because of intrinsic difficulties. Preliminary observations also suggest that the intact cerebellum or neocortex can be similarly kept in vitro.

This preparation will be extremely useful in a wide range of domains in neurobiology, notably for the study of generation and propagation of network-driven rhythmic activities and their roles in the formation of functional units. It can be combined with a variety of tracer and gene transfer techniques (Moriyoshi et al., 1996), as well as antisense knockdown techniques, to study the development of neuronal connections in vitro and its physiological correlates. Our preliminary results indicate that this preparation can also be used in neonatal mice, thus enabling the study of the consequences of genetic knockout. The maturation of intrinsic and extrinsic synaptic connections of the hippocampus as well as brain

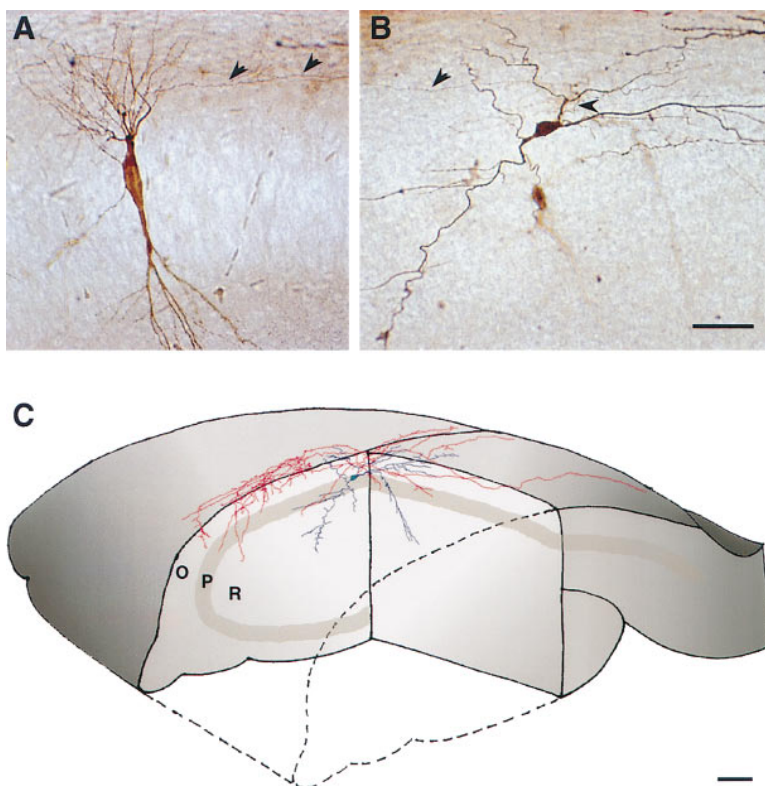


Figure 5. Morphological Characteristics and 3-D Reconstruction of Biocytin-labeled Neurons in P7 Rat IHFs Maintained In Vitro for 8 Hours

(A–B) Biocytin detection on 100 μm thick sections demonstrates the labeling of the soma, dendritic arborization, and axon (arrows) of a pyramidal neuron (A) and an interneuron (B) in the CA1 region.

(C) 3-D reconstruction of the biocytin-filled interneuron illustrated in (B). This interneuron displays a fusiform cell body located at the limit between stratum oriens and stratum pyramidale and gives rise to three primary dendrites that arborize in the stratum oriens, stratum pyramidale, and stratum radiatum of the CA1 region. The dendritic tree is mainly oriented in the transverse plane. This interneuron exhibits an axonal arborization that extends over 700 μm in the rostrocaudal plane, mainly in stratum oriens. Scale bars, 100 μm .

pathologies (notably ischemia and epilepsy) can be readily studied in the IHF, which can be kept for an extended period in vitro without any particular precaution and with a far better morphological preservation than in age-matched slices. Moreover, the use of the dual chamber will allow one to study distant effects of local pathological situations like ischemia or seizure in a model providing a better approximation of the in vivo situation.

Experimental Procedures

Preparation of Acute Intact Hippocampi

Intact hippocampal structures were obtained from neonatal and young (P0–P15) male Wistar rats. The rats were either cryoanesthetized (P0–P4 animals) or anesthetized with chloral hydrate (P5–15 animals; 350 mg/kg, intraperitoneally) and intracardially perfused with cold (0°C–4°C) oxygenated (95% O₂, 5% CO₂) modified ACSF containing sucrose (Hirsch et al., 1996). After decapitation, the brains were quickly removed and immersed for dissection into ice cold (2°C–4°C) oxygenated standard ACSF, which contained (in mM) 126 NaCl, 3.5 KCl, 2.0 CaCl₂, 1.3 MgCl₂, 25 NaHCO₃, 1.2 NaH₂PO₄, and 11 glucose. After removing the cerebellum and the most frontal part of the neocortex by coronal sectioning, the complex including the two hippocampi and the septum (Figure 6A) was isolated from surrounding structures by the following procedure: brainstem, mid-brain, and striatum were gently dissociated from the hippocampus with two spatulas. Neocortex was then removed by sliding along the corpus callosum, at the dorsal hippocampal and septal surfaces, a spatula initially inserted into the lateral ventricle. Great care was given to avoid damage of connections between structures. The IHFs could then be easily isolated from the septo-hippocampal complex. Another, more convenient way to prepare single IHFs was to split the hemispheres at the beginning of the dissection. Small pieces of surrounding tissue could be kept to allow insertion of needles for fixation of IHF in the recording chamber. For recordings of the two connected hippocampi in the dual chamber (Figure 6B), the

septum was always removed to allow tighter Vaseline contact with commissural connections and therefore better isolation between the two chambers (see below). The complete dissection procedure took 8–15 min. Careful dissection was found to be more important than speed for a healthy preparation. The septo-hippocampal complex or the IHFs were then gently transferred to a beaker containing oxygenated ACSF and kept at room temperature (20°C–22°C) for at least 1–2 hr before use.

As illustrated in Figure 3A, IHFs were then transferred to a fully submerged chamber (diameter, 1.2 cm; depth, 4 mm; bottom covered by sylgard), laid on a nylon mesh, fixed with entomological needles inserted through the surrounding tissue to sylgard, and superfused at a rate of 5–6 ml/min with oxygenated ACSF (30°C–32°C). The IHF was usually laid down on its ventral side in order to allow direct access to CA1 and CA3 regions. In the transilluminated IHF, the CA3 pyramidal layer could be easily distinguished as a thin light band (see Figure 6A). Interconnected hippocampi could also be perfused independently in a double recording chamber. The hippocampi were placed in the different compartments of the chamber so that the commissural connections were positioned in the narrow channel joining both compartments. Vaseline was then used to fill the channel, using an approach similar to that used for the spinal chord by Cazalets et al. (1996). While preserving functional commissural connections, this provided tight isolation between the two chambers, preventing the diffusion of drugs from one chamber to the other (Figure 6B).

For additional morphological experiments, 16 P0–P15 rats were similarly anesthetized and perfused, and 400 μm thick hippocampal slices were cut with a Leica VT 1000E (Germany) tissue slicer.

Morphological techniques

Light Microscopy

TISSUE PREPARATION. Sixteen IHFs (P0, P5, P10, and P15; $n = 4$ for each age) and 16 age-matched slices ($n = 4$ for each age) were processed for cresyl violet staining and immunohistochemistry after 4 hr ($n = 2$ for each age) or 10 hr ($n = 2$ for each age) of electrophysiological recordings, and 20 IHFs from P0–P15 neonatal or young rats were processed for biocytin detection. All IHFs and 400 μm thick

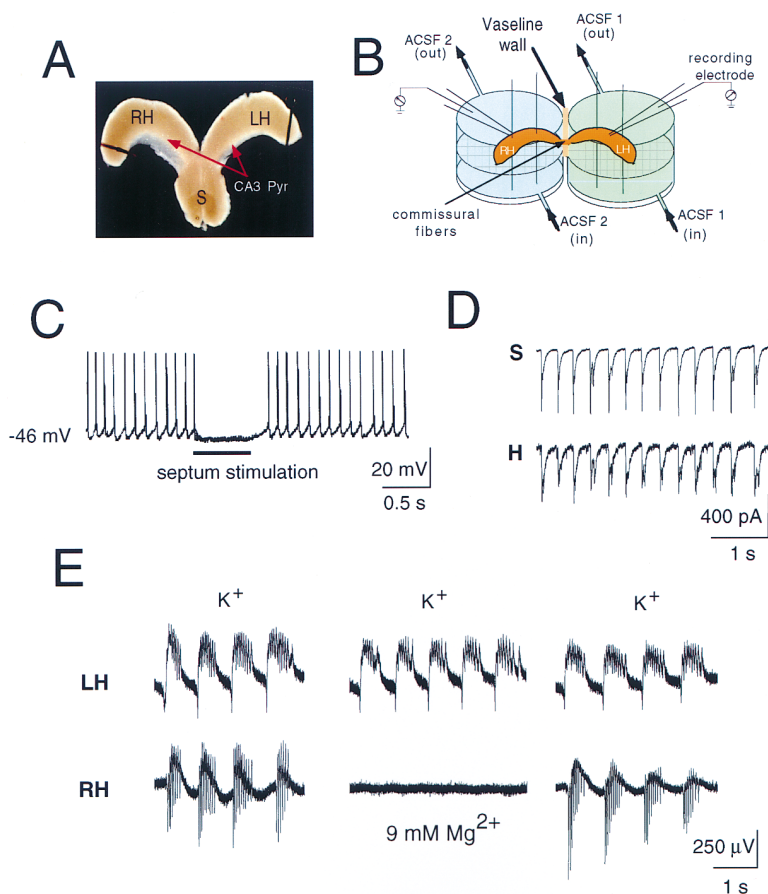


Figure 6. Septo-Hippocampal Complex and Two Connected Hippampi In Vitro

(A) Photomicrograph of the isolated septo-hippocampal complex. The CA3 pyramidal layer can be recognized as a thin light band (red arrows). RH, right hippocampus; LH, left hippocampus; S, septum.

(B) Scheme of the dual chamber that enables independent perfusion of the connected hippocampi. Vaseline wall separates the two compartments of the chamber, while preserving the commissural connections between the hippocampi.

(C–D) Septo-hippocampal recordings.

(C) During a long depolarizing pulse, the interneuron fired nonaccommodating action potentials. Electrical stimulation (40 Hz) in the septum hyperpolarized and inhibited the firing of the interneuron. Current-clamp recordings (internal solution 1).

(D) Synchronous epileptiform activity of neurons in septum (S) and hippocampus (H) during the ictal-like discharge induced by bath application of kainic acid (250 nM). Whole-cell, voltage-clamp recordings (internal solution 2).

(E) Field recordings from CA1 stratum radiatum in left (LH, upper traces) and right (RH, lower traces) connected hippocampi independently perfused with different ACSFs in the dual chamber presented in (B). Bath application of high K^+ (7.5 mM) solution to the left hippocampus generates synchronized ictal-like discharges in both hippocampi (left traces). Perfusion of the right hippocampus with high Mg^{2+} ACSF (middle traces) selectively blocks the paroxysmal activity in the right hippocampus in a reversible manner (15 min after wash of high Mg^{2+} ACSF; right traces).

slices were fixed in a solution of 4% paraformaldehyde in 0.1 M phosphate buffer (PB, pH 7.4) overnight at 4°C. After fixation, they were rinsed in PB for 1.5 hr, cryoprotected in a 30% sucrose solution overnight at 4°C, embedded in O.C.T. medium (Tissue-Tek), and quickly frozen on dry ice. Free-floating sections, 40 μ m thick to be processed for cresyl violet stainings and immunohistochemistry, or 100 μ m thick to be processed for biocytin detection, were cut in a transverse plane on a cryostat and collected in phosphate-buffered saline (0.1 M PBS, pH 7.4).

IMMUNOHISTOCHEMISTRY. Sections were processed for GAD67 immunohistochemistry by means of unlabeled polyclonal antiserum K2 (Kaufman et al., 1991) and standard avidin-biotin immunolabeling methods (Vectastain Elite ABC; Vector Laboratories, Burlingame, CA) according to previously described protocols (Esclapez et al., 1994).

BIOCYTIN-FILLED NEURONS AND 3-D RECONSTRUCTION. All adjacent sections from the whole hippocampal structure were processed for biocytin detection. Sections were incubated for 30 min in 1% H_2O_2 to block endogenous peroxidase, rinsed in 0.1 M PBS, and incubated for 20 hr in an avidin-biotin-peroxidase solution (1:100) prepared in 0.1 M PBS containing 0.3% Triton X-100. Sections were then processed for 15 min with 0.06% 3,3'-diaminobenzidine HCl and 0.006% H_2O_2 diluted in PBS, rinsed in PBS, mounted on gelatin-coated slides, dried, and coverslipped in an aqueous mounting medium (Crystal/Mount, Biomed). Biocytin-labeled neurons with their complete dendritic and axonal arborizations were reconstructed from serial adjacent sections with the NeuroLucida System (MicroBrightfield, Colchester, VT).

Electron Microscopy

After 4 hr in vitro, 8 IHFs (P0, P5, P10, and P15; $n = 2$ for each age) and 12 age-matched slices ($n = 3$ for each age) were fixed in a

solution of 4% paraformaldehyde and 1.5% glutaraldehyde in PB overnight at 4°C. After fixation, blocks of IHFs (500 μ m thick) were cut on a transverse plane. Blocks of hippocampus and slices were postfixed in 1% osmium tetroxide for 2 hr. After several rinses in PB, they were dehydrated and embedded in Epon-araldite resin. Polymerizations were obtained at 60°C in 48 hr. Thick (1–2 μ m) and ultrathin (100–200 nm) sections were cut on a Reichert ultramicrotome. Thick sections were stained with toluidine blue for light microscopy. Ultrathin sections were poststained with an aqueous solution of uranyl acetate and lead citrate and observed with a Philips EM 300 electron microscope.

Electrophysiological Recordings

Electrophysiological recordings were performed using the patch-clamp technique in the whole-cell configuration (Hamill et al., 1981) using Axopatch 200 (Axon Instrument, USA) and EPC-9 (List-Medical, Germany) patch-clamp amplifiers. Cells were patched either blindly or under visual control using infrared microscopy, with 7–10 M Ω microelectrodes containing (in mM) either 135 K gluconate, 2 MgCl₂, 0.1 CaCl₂, 1 EGTA, 2 Na₂ ATP, and 10 HEPES (pH 7.25) or 140 CsCl, 1 CaCl₂, 10 EGTA, 10 HEPES, and 2 Mg ATP (pH 7.25; osmolarity, 270–280 mmol/kg). Biocytin (0.5%) or Lucifer yellow (0.2%–0.4%) were routinely added to the pipette solution for morphological analysis.

Field potentials were recorded conventionally using glass micro-pipettes filled with ACSF (10–20 M Ω). Electrical stimulations (0–80 V, 10–30 μ s, delivered at 0.02–0.05 Hz) were provided by a bipolar electrode placed in the different areas of the IHF.

TMA⁺ and pH measurements were performed as described previously (Nicholson, 1983; Voipio et al., 1995).

Imaging

Infrared imaging was performed as described previously for slices (Stuart et al., 1993). The preparation was transilluminated on the stage of an Axioscope Karl Zeiss microscope (40× water-immersion objective lens; magnification, 400×) and Workbench software (Axon Instruments) with a filter of 730 nm. Lucifer yellow fluorescent images were monitored using Photonix monochromator at 450 nm and intensified Photonix CCD camera and Workbench software (Axon Instruments).

Ca²⁺ imaging experiments were performed as described previously (Leinekugel et al., 1997). In brief, neurons were loaded extracellularly by focal pressure application of Fluo 3-AM (30 μM). Fluorescence was monitored using a confocal laser scanning microscope BIORAD MRC 600, equipped with an argon-krypton laser (excitation, 488 nm) and photomultiplier (>500 nm collected), driven by the SOM program (BIORAD). Changes in fluorescence were analyzed off-line using the program Fluo (IMSTAR, France).

Drugs

Drugs used were purchased from Sigma (biocytin and tetrodotoxin), Tocris Neuramin (isoguvacine, bicuculline, CNQX, APV, and kainic acid), and Molecular Probes (Fluo 3-AM and Lucifer yellow).

Acknowledgments

We are grateful to Dr. C. Bernard for providing the conceptual input to generate this preparation, Dr. H. Gozlan for providing some of the field recording data, Drs. G. Holmes and K. Kaila for their suggestions, and D. Diabira and I. Jorquera for technical assistance. Financial support from INSERM, Fondation pour la Recherche Redicale, and the French Ministry of Research is acknowledged.

Received July 2, 1997; revised September 5, 1997.

References

- Aitken, P.G., Breese, G.R., Dudek, F.F., Edwards, F., Espanol, M.T., Larkman, P.M., Lipton, P., Newman, G.C., Nowak, T.S., Panizzon, K.L., et al. (1995). Preparative methods for brain slices: a discussion. *J. Neurosci. Methods* **59**, 139–149.
- Ben-Ari, Y., Cherubini, E., Corradetti, R., and Gaiarsa, J.L. (1989). Giant synaptic potentials in immature rat CA3 hippocampal neurons. *J. Physiol. (Lond.)* **416**, 303–325.
- Bourque, C.W., and Renaud, L.P. (1984). Activity patterns and osmosensitivity of rat superoptic neurons in perfused hypothalamic explants. *J. Physiol. (Lond.)* **349**, 631–642.
- Cazalets, J.-R., Borde, M., and Clarac, F. (1996). The synaptic drive from the spinal locomotor network to motoneurons in the newborn rat. *J. Neurosci.* **16**, 298–306.
- De Curtis, M., Pare, D., and Llinas, R. (1991). The electrophysiology of the olfactory hippocampal circuit in the isolated and perfused adult mammalian brain. *Hippocampus* **1**, 341–354.
- Dupuy, S.T., and Houser, C.R. (1996). Prominent expression of two forms of glutamate decarboxylase in the embryonic and early postnatal rat hippocampal formation. *J. Neurosci.* **16**, 6919–6932.
- Esclapez, M., Tillakaratne, N.J.K., Kaufman, D.L., Tobin, A.J., and Houser, C.R. (1994). Comparative localization of two forms of glutamic acid decarboxylase and their mRNAs in rat brain supports the concept of functional differences between the two forms. *J. Neurosci.* **14**, 1834–1855.
- Frank, E. (1993). New life in an old structure: the development of synaptic pathways in the spinal cord. *Curr. Opin. Neurobiol.* **3**, 82–86.
- Freund, T., and Antal, M. (1988). GABA-containing interneurons in the septum control inhibitory interneurons in the hippocampus. *Nature* **336**, 170–173.
- Freund, T.F., and Buszaki, G. (1996). Interneurons of the hippocampus. *Hippocampus* **6**, 347–470.
- Fulton, B.P., and Walton, K. (1986). Electrophysiological properties on neonatal rat motoneurons studied in vitro. *J. Physiol. (Lond.)* **370**, 651–680.
- Gu, X., and Spitzer, N.C. (1995). Distinct aspects of neuronal differentiation encoded by frequency of spontaneous Ca²⁺ transients. *Nature* **375**, 784–787.
- Hamill, O.P., Marty, A., Neher, E., Sakmann, B., and Sigworth, F.J. (1981). Improved patch-clamp techniques for high-resolution current recording from cell-free membrane patches. *Pflügers Arch.* **397**, 85–100.
- Hirsch, J.C., Quesada, O., Esclapez, M., Gozlan, H., Ben-Ari, Y., and Bernard, C. (1996). Enhanced NMDAR-dependent epileptiform activity is controlled by oxidizing agents in a chronic model of temporal lobe epilepsy. *J. Neurophysiol.* **76**, 4185–4189.
- Jacquin, T.D., Borday, V., Schneider-Maunoury, S., Topilko, P., Ghilini, G., Kato, F., Charnay, P., and Champagnat, J. (1996). Reorganization of pontine rhythmogenic neuronal networks in Krox-20 knock out mice. *Neuron* **17**, 747–758.
- Kaufman, D.L., Houser, C.R., and Tobin, A.J. (1991). Two forms of the gamma-aminobutyric acid synthetic enzyme glutamate decarboxylase have distinct intraneuronal distributions and cofactor interactions. *J. Neurochem.* **56**, 720–723.
- Khazipov, R., Leinekugel, X., Khalilov, I., Gaiarsa, J.L., and Ben-Ari, Y. (1997). Synchronization of GABAergic interneuronal network in CA3 subfield of neonatal rat hippocampal slices. *J. Physiol. (Lond.)* **498**, 763–772.
- Leinekugel, X., Medina, I., Khalilov, I., Ben-Ari, Y., and Khazipov, R. (1997). Ca²⁺ oscillations mediated by the synergistic excitatory actions of GABA_A and NMDA receptors in neonatal hippocampus. *Neuron* **18**, 243–255.
- Mooney, R., Penn, A.A., Gallego, R., and Schatz, C.J. (1996). Thalamic relay of spontaneous retinal activity prior to vision. *Neuron* **17**, 863–874.
- Moriyoshi, K., Richards, L.J., Akazawa, C., O'Leary, D.D.M., and Nakanishi, S. (1996). Labeling neuronal cells using adenoviral gene transfer of membrane-targeted GFP. *Neuron* **16**, 255–260.
- Muhlethaler, M., de Curtis, M., Walton, K., and Llinas, R. (1993). The isolated and perfused brain of the guinea-pig in vitro. *Eur. J. Neurosci.* **5**, 915–926.
- Nicholson, C. (1983). Ion-selective microelectrodes and diffusion measurements as tools to explore the brain cell microenvironment. *J. Neurosci. Methods* **48**, 199–213.
- O'Donovan, M.J. (1989). Motor activity in the isolated spinal cord of the chick embryo: synaptic drive and firing pattern of single motoneurons. *J. Neurosci.* **9**, 943–958.
- Otsuka, M., and Konishi, S. (1974). Electrophysiology of mammalian spinal cord in vitro. *Nature* **252**, 733–734.
- Pare, D., and Llinas, R. (1995). Intracellular study of direct entorhinal inputs to field CA1 in the isolated guinea-pig brain in vitro. *Hippocampus* **5**, 115–119.
- Peters, A., Palay, S.L., and de F. Webster, H. (1991). The fine structure of the nervous system. In *Neurons and Their Supporting Cells* (New York: Oxford University Press).
- Rozenberg, F., Robain, O., Jardin, L., and Ben-Ari, Y. (1989). Distribution of GABAergic neurons in late and early postnatal rat hippocampus. *Dev. Brain Res.* **50**, 177–187.
- Stuart, G.J., Dodt, H.-U., and Sakmann, B. (1993). Patch-clamp recordings from the soma and dendrites of neurons in brain slices using infrared video microscopy. *Pflügers Arch.* **423**, 511–518.
- Toth, K., Freund, T., and Miles, R. (1997). Disinhibition of rat hippocampal pyramidal cells by GABAergic afferents from the septum. *J. Physiol. (Lond.)* **500**, 463–474.
- Tremblay, E., Nitecka, L., Charton, G., Bouillot, J.P., Berger, M., and Ben-Ari, Y. (1984). Maturation of kainic acid seizure-brain damage syndrome in the rat. I. Motor, electrographic and metabolic observations. *Neuroscience* **13**, 1051–1072.
- Voipio, J., Paalasmaa, P., Taira, T., and Kaila, K. (1995). Pharmacological characterization of extracellular pH transients evoked by selective synaptic and exogenous activation of AMPA, NMDA, and GABA_A receptors in the rat hippocampal slice. *J. Neurophysiol.* **74**, 633–642.